

Cutoff-free Circuit Quantum Electrodynamics

Moein Malekakhlagh, Alexandru Petrescu, and Hakan E. Türeci

Department of Electrical Engineering, Princeton University, Princeton, New Jersey, 08544

(Dated: August 18, 2017)

Any quantum-confined electronic system coupled to the electromagnetic continuum is subject to radiative decay and renormalization of its energy levels. When coupled to a cavity, these quantities can be strongly modified with respect to their values in vacuum. Generally, this modification can be accurately captured by including only the closest resonant mode of the cavity. In the circuit quantum electrodynamics architecture, it is however found that the radiative decay rates are strongly influenced by far off-resonant modes. A multimode calculation accounting for the infinite set of cavity modes leads to divergences unless a cutoff is imposed. It has so far not been identified what the source of divergence is. We show here that unless gauge invariance is respected, any attempt at the calculation of circuit QED quantities is bound to diverge. We then present a theoretical approach to the calculation of a finite spontaneous emission rate and the Lamb shift that is free of cutoff.

Introduction. An atom-like degree of freedom coupled to continuum of electromagnetic (EM) modes spontaneously decays. When the atom is confined in a resonator, the emission rate can be modified compared with its value in free space, depending on the EM local density of states at the atomic position [1–4], which is called the Purcell effect [5]. An accompanying effect is the Lamb shift, a radiative level shift first observed in the microwave spectroscopy of the hydrogen ${}^2P_{1/2} - {}^2S_{1/2}$ transition [6]. These quantities have been experimentally accurately characterized for superconducting Josephson junction (JJ) based qubits coupled to coplanar transmission lines [7, 8] and three-dimensional resonators [9]. In the dispersive regime where a qubit with transition frequency ω_j is far-detuned from the nearest resonant cavity mode (frequency ν_r , loss κ_r), single mode expressions exist for the Purcell decay rate, $\gamma_P = (g/\delta)^2 \kappa_r$ and the Lamb shift, $\Delta_L = g^2/\delta$. Here g denotes the coupling between the qubit and the cavity mode and $\delta = \omega_j - \nu_r$ denotes their detuning [10]. However, for large couplings accessible in circuit QED, the single mode approximation is often inaccurate [7, 8]. In addition, due to particular boundary conditions imposed by the capacitive coupling of a resonator to external waveguides, the qubit relaxation time is limited by the EM modes that are far-detuned from the qubit frequency [8]. Similarly the measured Lamb shift in the dispersive regime can only be accurately fit with an extended Jaynes-Cummings (JC) model including several modes and qubit levels [7]. The Purcell rate has been generalized to account for all modes

$$\gamma_P = \sum_n (g_n/\delta_n)^2 \kappa_n, \quad (1)$$

where g_n and $\delta_n = \omega_j - \nu_n$ are coupling to and detuning from resonator mode n with frequency ν_n and decay rate κ_n . Expression (1) is divergent without imposing a high-frequency cutoff [8]. Divergences appear as well in the Lamb shift and other vacuum-induced phenomena, e.g. photon-mediated qubit-qubit interactions [11]. These divergences are neither specific to the dispersive limit nor to the calculational scheme used to compute QED quan-

ties. This issue is well-known for the Lamb shift [6], but less noted for the spontaneous emission rate. Indeed, free space spontaneous emission rate diverges as well, as we show in [12]. The finite result by Wigner and Weisskopf [13, 14] is due to Markov approximation which filters out the ultraviolet divergence. Recent generalizations of the Wigner-Weisskopf approach impose an artificial cut-off to obtain a finite result [15]. So far, no satisfactory theoretical explanation has been given for these divergences. Here we address this issue within the framework of circuit quantum electrodynamics [16] (QED) and show that finite expressions can be obtained when gauge invariance is respected. We focus here on a superconducting artificial atom coupled to an open transmission-line resonator, but our results should be valid for other types of one-dimensional open EM environments as well.

Gauge invariance in circuit QED. The role of gauge invariance in accounting for light-matter interaction has been a vexing question since the beginnings of QED (see Ref. [17], and references therein). Hence, we first discuss gauge invariance in superconducting electrical circuits, and its impact on QED observables.

We consider a weakly nonlinear charge qubit (e.g. transmon [18][19]) capacitively coupled to a transmission-line resonator that in turn is coupled at both ends to semi-infinite waveguides (Fig. 1a). We assign flux variables to nodes, $\Phi_n(t) = \int^t d\tau V_n(\tau)$, with $V_n(t)$ being the instantaneous voltage at node n with respect to the ground node [16, 20]. Fixing the ground amounts to a particular gauge choice [16]. For the connection geometry in Fig 1a, the light-matter interaction derives from the energy on the coupling capacitor in the dipole approximation, $T_{\text{int}} = \frac{1}{2} C_g [\dot{\Phi}(x_0) - \dot{\Phi}_j]^2$ [12], with x_0 the qubit position. If from the three terms in its expansion, $T_{\text{EM}} = \frac{1}{2} C_g \dot{\Phi}(x_0)^2$, $T_{\text{EM-JJ}} = -C_g \dot{\Phi}(x_0) \cdot \dot{\Phi}_j$ and $T_{\text{JJ}} = \frac{1}{2} C_g \dot{\Phi}_j^2$, only the direct interaction $T_{\text{EM-JJ}}$ is kept, a multimode JC model in terms of circuit parameters can be derived [21], but gives rise to a diverging Purcell rate using Eq. (1). This open JC Model involves a two level approximation (TLA) of the JJ Hilbert space, the rotating wave approximation (RWA) to drop nonresonant contributions, and the Born and Markov approximations

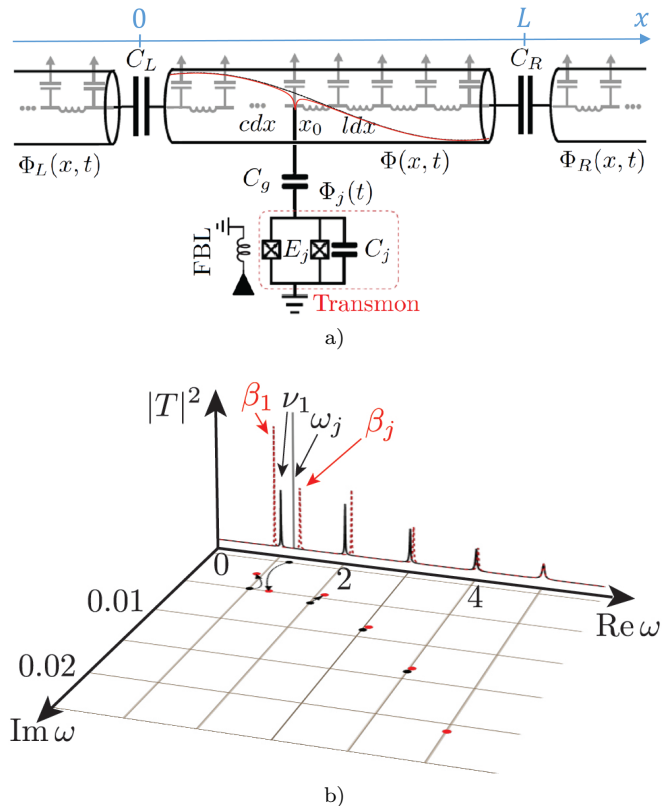


FIG. 1. a) A transmon qubit coupled to an open superconducting resonator. The black dashed line is a cartoon of the fundamental bare mode of the resonator, while the red solid curve represents the modified resonator mode. b) The transmission $|T|^2$ is shown versus the real frequency for the bare resonator modes (solid black curves). Capacitively coupling the qubit, whose transition frequency ν_j is slightly above the fundamental resonator frequency ν_1 , gives rise to hybridized modes (dashed red curves). Alternatively, one may study the positions of these resonances in the complex frequency plane, where the bare resonator and qubit poles (black points) are displaced into hybridized resonator-like and qubit-like resonances (red points). The Purcell decay and the Lamb shift are obtained as the displacement of the qubit-like pole. The bare (hybridized) complex frequencies are the poles (zeros) of the characteristic function $D_j(s)$.

leading to a Master equation accounting for losses due to resonator-waveguide coupling. It is unclear which approximation underlies the divergence, or whether the divergence can be resolved within the effective subgap circuit QED field theory.

We first note that keeping only the direct interaction $T_{\text{EM-JJ}}$ violates gauge invariance. We find that inclusion of all terms, in particular T_{EM} , equivalent to the diamagnetic A^2 term in the minimal coupling Hamiltonian $(p - eA)^2/2m$ [22], is essential to make all studied QED observables finite.

The A^2 -term is thought to have no impact on transition frequencies in vacuum-induced effects such as the Lamb shift. Because it does not involve atomic operators,

it is expected to make the same perturbative contribution to every atomic energy level, precluding observable shifts in *transition* frequencies [23]. This argument relies on perturbation theory in the A^2 -term. We show that the diamagnetic term *does* have an impact when accounted for exactly to all orders.

Heisenberg equations of motion describing the infinite network in Fig. 1a, extending from $x = -\infty$ to $x = \infty$, are [12, 24]

$$\hat{\varphi}_j(t) + (1 - \gamma)\omega_j^2 \sin[\hat{\varphi}_j(t)] = \gamma\partial_t^2 \hat{\varphi}(x_0, t), \quad (2)$$

$$[\partial_x^2 - \chi(x, x_0)\partial_t^2] \hat{\varphi}(x, t) = \chi_s\omega_j^2 \sin[\hat{\varphi}_j(t)]\delta(x - x_0) \quad (3)$$

Here $\hat{\varphi}_j(t)$ and $\hat{\varphi}(x, t)$ are dimensionless flux operators for the JJ and the resonator-waveguide system, respectively, $\gamma \equiv C_g/(C_g + C_j)$ is a capacitive ratio, $\chi_s = \gamma C_j/cL$ is the dimensionless series capacitance of C_g and C_j , ω_j is the dimensionless transmon frequency, and $\chi_i \equiv C_i/(cL)$ for $i = g, j, R, L$ [12]. These two inhomogeneous equations show that the flux field at x_0 drives the dynamics of the JJ [Eq. (2)], while the JJ acts as a source driving the EM fields [Eq. (3)]. In addition, the fields are subject to continuity conditions at the ends of the resonator $x = 0, 1$ (in units of L).

It is instructive to trace the individual terms of T_{int} in Eqs. (2-3). T_{JJ} modifies the qubit frequency, renormalizing γ from C_g/C_j to $C_g/(C_g + C_j)$, while the direct interaction term $T_{\text{EM-JJ}}$ gives source terms in both equations. Most importantly, T_{EM} introduces an effective scattering term in the wave equation describing the fields in the transmission line, by modifying the unitless capacitance per length from 1 to $\chi(x, x_0) = 1 + \chi_s\delta(x - x_0)$. Consequently, these equations are consistent [22] with Kirchhoff's law of current conservation. In particular, at $x = x_0$, Eq. (3) yields $\partial_x \hat{\varphi}(x, t)|_{x_0^-}^+ = \chi_s\partial_t^2 \hat{\varphi}(x_0, t) + \chi_s\omega_j^2 \sin[\hat{\varphi}_j(t)]$, where the discontinuity in the resonator current is equal to the total current through the capacitive and Josephson branches of the transmon. Similar modification of resonator dynamics has been pointed out before for JJ-based qubits [9, 22, 25].

Equation 3 can be solved in the Fourier domain, where $\hat{\varphi}(x, \omega) = \int_{-\infty}^{\infty} dt \hat{\varphi}(x, t)e^{-i\omega t}$ can be expanded in the basis $\tilde{\varphi}_n(x, \omega)$ that solves the generalized eigenvalue problem $[\partial_x^2 + \chi(x, x_0)\omega^2] \tilde{\varphi}_n(x, \omega) = 0$, subject to continuity conditions at the ends of the resonator, i.e. $\partial_x \tilde{\varphi}_n(1^-, \omega) = \chi_R\omega^2[\tilde{\varphi}_n(1^-, \omega) - \tilde{\varphi}_n(1^+, \omega)]$ and $\partial_x \tilde{\varphi}_n(0^+, \omega) = \chi_L\omega^2[\tilde{\varphi}_n(0^-, \omega) - \tilde{\varphi}_n(0^+, \omega)]$, which models the coupling to the waveguides and associated loss. The Dirac δ -function in $\chi(x, x_0)$ leads to the discontinuity

$$-\partial_x \tilde{\varphi}_n(x)|_{x_0^-}^+ = \chi_s\omega_n^2 \tilde{\varphi}_n(x_0), \quad (4)$$

resulting in a modified current-conserving (CC) basis [22]. These modifications in the spectrum of the transmission line resonator impact the qubit dynamics that is driven by resonator fluctuations.

The role of modal modification in Eq. (4) can be illustrated with a phenomenological model. Previously, the Purcell rate and the Lamb shift have been calculated using the Lindblad formalism in the dispersive limit [10]. An effective multimode JC model

$$\hat{\mathcal{H}}_{\text{JC}} = \frac{\omega_j}{2} \hat{\sigma}_z + \sum_n \nu_n \hat{a}_n^\dagger \hat{a}_n + \sum_n g_n (\hat{\sigma}^+ \hat{a}_n + \hat{\sigma}^- \hat{a}_n^\dagger) \quad (5)$$

can be obtained from our first principles model [12], which incorporates the modifications to the resonator modes and the qubit dynamics. Resonator losses are included through a Bloch–Redfield equivalent zero-temperature master equation for the reduced density matrix of the resonator and qubit $\hat{\rho} = -i[\hat{\mathcal{H}}_{\text{JC}}, \hat{\rho}] + \kappa_n (2\hat{a}_n \hat{\rho} \hat{a}_n^\dagger - \{\hat{\rho}, \hat{a}_n^\dagger \hat{a}_n\})$. The expressions of cavity frequencies ν_n , associated losses κ_n and modal interaction strengths g_n are given in the Supplementary Material [12]. All these quantities are functions of χ_s , the strength of the modification of the capacitance per unit length. In particular, the light-matter coupling is found as $g_n = \frac{1}{2} \gamma \sqrt{\chi_j} \sqrt{\omega_j \nu_n} \hat{\varphi}_n(x_0)$. We show in Fig. 2a that g_n is non-monotonic [22] for any $\chi_s \neq 0$, first increasing, then turning over at a critical χ_s -dependent mode n , decreasing as $g_n \sim 1/\sqrt{n}$ in the large- n limit [12]. This high frequency behavior of g_n renders the multimode Purcell rate finite, without an imposed cutoff [26].

This phenomenon is not specific to the resonator geometry in Fig. 1a. The underlying physics is the conservation of current at the position x_0 of the qubit. At high frequency, the series capacitance χ_s becomes a short-circuit to ground, acting as a low-pass filter and suppressing mode amplitude at x_0 . This is the cause of the power law drop of g_n as $n \rightarrow \infty$ (Fig. 2a). Moreover, eliminating the continuum degrees of freedom of the waveguides gives an effective decay rate for each mode, κ_n , which increases monotonically as $\kappa_n \sim n^{0.3}$ (Fig. 2b). In the Supplementary Material, we show that for $\chi_s = 0$ the resulting series Eq. (1) diverges [12], as pointed out in previous studies [8, 11]. For *any* nonzero χ_s , individual terms in the sum (1) display a universal power law $\sim n^{-2.7}$ (Fig. 2c), which guarantees convergence [27].

Solution of the Heisenberg-Langevin equations. Although we showed that the expression (1) for the Purcell decay rate converges, it is only valid in the dispersive regime $g_n \ll \delta_n$. This estimate for the Purcell decay rate and the Lamb shift will deviate substantially from the exact result for a range of order g_n around each cavity resonance, diverging as the qubit frequency approaches the resonance (see Fig. 3). This fictitious divergence can in principle be cured by solving the full multimode Master equation. Even if computational challenges relating to the long-time dynamics in such a large Hilbert space can be addressed, the resulting rate would still be subject to the TLA, RWA, Born and Markov approximations, casting a priori an uncertainty on its reliability.

An improved analytic result that is uniformly valid in the transmon frequency, and is not limited by the aforementioned approximations can be found by solving

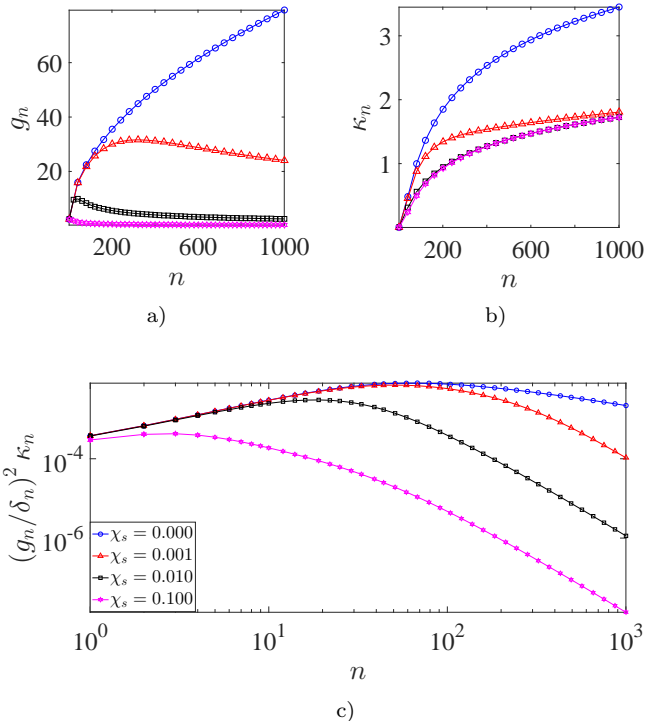


FIG. 2. (Color online) Dependence of a) coupling strength g_n , b) resonator decay rate κ_n (See [12] for derivation) and c) Purcell decay rate in the dispersive regime $(g_n/\delta_n)^2 \kappa_n$ on mode number n for different values of $\chi_s = \{0, 10^{-3}, 10^{-2}, 10^{-1}\}$. Other parameters are set as $\chi_R = \chi_L = 10^{-3}$ and $x_0 = 0^+$.

Eqs. (2-3) perturbatively in the transmon's weak nonlinearity. EM degrees of freedom can be integrated out by solving Eq. (3) exactly, plugging into Eq. (2) and tracing over the photonic Hilbert space. To lowest order in the transmon nonlinearity $\epsilon = (E_c/E_j)^{1/2}$, where E_c and E_j are the charging and Josephson energy, respectively, the effective equation for the qubit is [24]

$$\begin{aligned} \hat{X}_j(t) + \omega_j^2 [1 - \gamma + i\mathcal{K}_1(0)] \hat{X}_j(t) \\ = -\omega_j^2 \int_0^t dt' \mathcal{K}_2(t-t') \hat{X}_j(t'), \end{aligned} \quad (6)$$

where $\hat{X}_j(t) = \text{Tr}_{ph} \{ \hat{\rho}_{ph}(0) \hat{\varphi}_j(t) \} / \phi_{\text{zpf}}$ is the reduced flux operator traced over the photonic degrees of freedom and $\phi_{\text{zpf}} \equiv (\sqrt{2}\epsilon)^{1/2}$ is the magnitude of the zero-point phase fluctuations. This delay equation features the memory kernels $\mathcal{K}_n(\tau) \equiv \gamma \chi_s \int_{-\infty}^{+\infty} \frac{d\omega}{2\pi} \omega^n G(x_0, x_0, \omega) e^{-i\omega\tau}$, where $G(x, x', \omega)$ is the classical EM Green's function defined by $[\partial_x^2 - \chi(x, x_0) \partial_t^2] G(x, x', \omega) e^{-i\omega t} = e^{-i\omega t} \delta(x - x')$ implying that $G(x, x', \omega)$ is the amplitude of the flux field created at x by a transmon oscillating with a frequency ω at x' [24]. The term on the right hand side of 6 is therefore proportional to the fluctuating current driving the qubit at time t , that was excited by itself at an earlier time t' . This Green's function correctly encodes

the modification of the capacitance per length. Equation (6) can be solved exactly in the Laplace domain

$$\hat{X}_j(s) = \frac{s\hat{X}_j(0) + \hat{X}_j(0)}{D_j(s)}, \quad (7)$$

where $\tilde{h}(s) \equiv \int_0^\infty dt h(t) e^{-st}$, with $D_j(s)$ defined as [24]

$$D_j(s) \equiv s^2 + \omega_j^2 \left[1 - \gamma + i\mathcal{K}_1(0) + \tilde{\mathcal{K}}_2(s) \right]. \quad (8)$$

We express the characteristic function $D_j(s)$ in meromorphic form

$$D_j(s) = (s - p_j)(s - p_j^*) \prod_m \frac{(s - p_m)(s - p_m^*)}{(s - z_m)(s - z_m^*)}. \quad (9)$$

The poles of $1/D_j(s)$ are the hybridized qubit-like and resonator-like complex-valued excitation frequencies, $p_j \equiv -\alpha_j - i\beta_j$ and $p_n \equiv -\alpha_n - i\beta_n$, respectively, of the qubit-resonator system, while its zeroes $z_n \equiv -i\omega_n = -\kappa_n - i\nu_n$ correspond to bare non-Hermitian [12] cavity resonances. The real part of the qubit-like pole, α_j , is the Purcell loss rate, while $\beta_j - \omega_j$ is the Lamb shift, as shown in Fig. 1b. In the Supplementary Material, we show that $D_j(s)$ is convergent, and hence so are all hybridized frequencies, for any nonzero χ_s .

The A^2 -term kept in our calculation to enforce gauge invariance plays the role of the ‘‘counterterm’’ discussed by Caldeira and Leggett to cancel infinite frequency renormalization [28, 29]. This problem has also been discussed in the context of the quantum theory of laser radiation [30].

Perturbative corrections. The transmon nonlinearity neglected in Eq. (6) can be reintroduced as a weak perturbation. The leading order correction to the hybridized resonances amounts to self- and cross-Kerr interactions [9, 25]. Using multi-scale perturbation theory [24, 32], the correction to the transmon qubit-like resonance β_j is given by

$$\hat{\beta}_j = \beta_j - \frac{\sqrt{2}\epsilon}{4} \omega_j \left[u_j^4 \hat{\mathcal{H}}_j(0) + \sum_n 2u_j^2 u_n^2 \hat{\mathcal{H}}_n(0) \right] \quad (10)$$

where the coefficients $u_{j,n}$ define the transformation from the hybridized to the unhybridized modes and $\hat{\mathcal{H}}_{j,n}(0)$ are the free Hamiltonians of the transmon and mode n , respectively. For $\chi_g \rightarrow 0$, we find $u_j \rightarrow 1$, $u_n = 0$ and $\beta_j \rightarrow \omega_j$ such that we recover the frequency correction of free quantum Duffing oscillator $\hat{\omega}_j = \omega_j [1 - \frac{\sqrt{2}\epsilon}{4} \hat{\mathcal{H}}_j(0)]$ [33]. We note three features of this result. Firstly, the correction is an operator and that expresses the fact that transmon levels are anharmonic. The anharmonicity can be calculated from the expectation value of a corrected quadrature operator [12]. Secondly, by virtue of the lowest order result being convergent without a cutoff, the perturbative corrections are also convergent in the number of modes included. Finally, this result is not limited

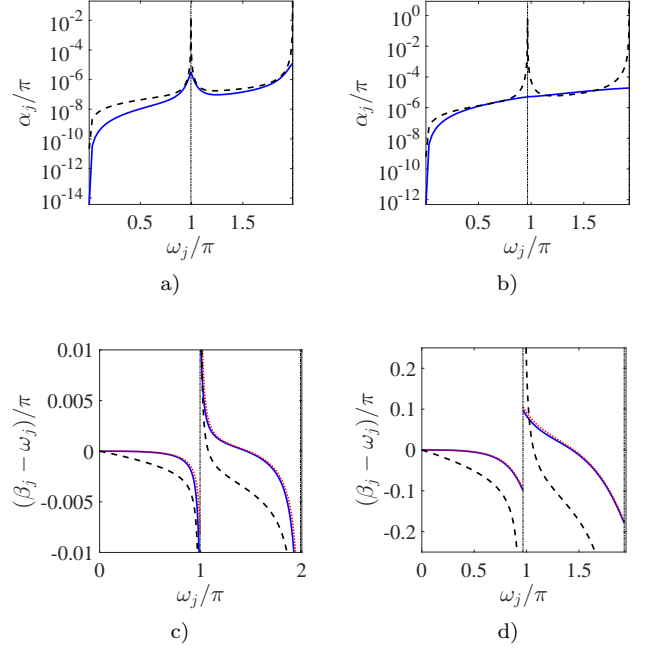


FIG. 3. (Color online) Comparison of a,b) spontaneous decay rate between the linear theory (blue solid) and the dispersive limit result γ_P (black dashed) as a function of ω_j . c,d) Lamb shift between the linear theory (blue solid), leading order perturbation (red dotted) and the dispersive limit result Δ_L (black dashed). a,c) $\chi_g = 0.001$ and b,d) $\chi_g = 0.1$. Both values of χ_g are in strong coupling regime, i.e. $g_1/\alpha_j \gg 1$. However, $\chi_g = 0.1$ ($g_1/\nu_1 = 0.1033$) reaches ultrastrong coupling [31], where multimode effects are non-negligible. The nonlinearity is set as $\epsilon = 0.1$, while other parameters are $\chi_R = \chi_L = 10^{-3}$ and $\chi_j = 0.05$. The vertical dash-dotted black line shows the position of the fundamental frequency of the resonator.

by the qubit-resonator coupling strength or the openness of the cavity. The final result is finite for all qubit frequencies, as opposed to the dispersive-limit result. The correction to the Purcell decay is higher order and forms the subject of future work.

We compared the spontaneous decay from the linear theory (blue solid) to the dispersive limit estimate γ_P in Eq. (1) (black dashed) as the transmon frequency is tuned across the fundamental mode in Figs. 3a-3b. First, the spontaneous decay is asymmetric, since there are (in)initely many modes with frequency (larger) smaller than ω_j . This feature is captured by both theories. Second, the spontaneous decay is enhanced as the qubit frequency approaches the fundamental resonator frequency. However, the dispersive limit estimate is perturbative in g_n/δ_n and hence yields a divergent result (fake kink) on resonance regardless of coupling constant, contrary to our result 9 which predicts a finite value even at ultrastrong coupling (Fig. 3b and caption).

In Figs. 3c-3d we compare the Lamb shift from the linear theory (blue solid) and the leading order pertur-

bation theory (red dotted) to the dispersive multimode estimate (black dashed) $\sum_n g_n^2/\delta_n$ [10]. Below the fundamental mode, the Lamb shift is negative due to the collective influence of all higher modes that redshifts the qubit frequency. Above the fundamental mode, there appears a competition between the hybridization with the fundamental mode and all higher modes. Close enough to the fundamental mode, the Lamb shift is positive until it changes sign, as predicted by all three curves.

Conclusion. We have presented a framework to calculate the spontaneous decay and the Lamb shift of a transmon qubit, convergent in the number of resonator modes without the need for rotating-wave, two-level, Born or Markov approximations, or a high frequency cutoff. This is achieved by an *ab initio* treatment of the quantum circuit equations of motion containing the A^2 -term to enforce gauge invariance. Therefore, the modes of the resonator are modified such that the light-matter coupling is suppressed at high frequencies. Formulating the cavity resonances in terms of non-Hermitian modes provides access to the spontaneous decay, the Lamb shift, and any other QED observables in a unified way.

Acknowledgements. We acknowledge helpful discussions with Zlatko Mineev and S. M. Girvin. This work was supported by the US Department of Energy, Office of Basic Energy Sciences, Division of Materials Sciences and Engineering, under Award No. de-sc0016011.

Note. While finishing this manuscript we became aware of Ref. 34, which arrives at a similar conclusion for the Lamb shift in the dispersive regime through a different approach.

Supplementary Material: Cutoff-free Circuit Quantum Electrodynamics

I. HEISENBERG EQUATIONS OF MOTION

In this section, we present the Heisenberg equations of motion in terms of flux variables [20, 35]. These equations were derived before by the authors [24] (see App. A), but the main steps are summarized below for clarity. The flux variable is defined at any node n in terms of the voltage at that node with respect to a fixed ground node

$$\Phi_n(t) \equiv \int_0^t dt' V_n(t'). \quad (11)$$

The classical Lagrangian is the sum of the Lagrangians for the Josephson junction, resonator, right and left waveguides, capacitive coupling between the resonator and the waveguides and the transmon-resonator capacitive coupling, respectively (let $U_j(\Phi_j)$ be the nonlinear Josephson potential):

$$\begin{aligned} \mathcal{L} = & \underbrace{\frac{1}{2}C_j\dot{\Phi}_j(t)^2 - U_j(\Phi_j(t))}_{\mathcal{L}_j} \\ & + \underbrace{\int_{0^+}^{L^-} dx \left[\frac{1}{2}c(\partial_t\Phi)^2 - \frac{1}{2l}(\partial_t\Phi)^2 \right]}_{\mathcal{L}_{\text{Res}}} \\ & + \underbrace{\int_{L^+}^{\infty} dx \left[\frac{1}{2}c(\partial_t\Phi_R)^2 - \frac{1}{2l}(\partial_x\Phi_R)^2 \right]}_{\mathcal{L}_{\text{RW}}} \\ & + \underbrace{\int_{-\infty}^{0^-} dx \left[\frac{1}{2}c(\partial_t\Phi_L)^2 - \frac{1}{2l}(\partial_x\Phi_L)^2 \right]}_{\mathcal{L}_{\text{LW}}} \\ & + \underbrace{\frac{1}{2}C_L \left[\dot{\Phi}_L(0^-, t) - \dot{\Phi}(0^+, t) \right]^2}_{\mathcal{L}_{C_L}} \\ & + \underbrace{\frac{1}{2}C_R \left[\dot{\Phi}_R(L^+, t) - \dot{\Phi}(L^-, t) \right]^2}_{\mathcal{L}_{C_R}} \\ & + \underbrace{\frac{1}{2}C_g \left[\dot{\Phi}_j(t) - \dot{\Phi}(x_0, t) \right]^2}_{\mathcal{L}_{C_g}}, \end{aligned} \quad (12)$$

From Eq. (12) one can derive, via a Legendre transformation followed by quantization [16, 20, 36], the Hamiltonian operator associated with the quantum circuit. The quantum Hamiltonian for $C_{R,L} \rightarrow 0$ is in Ref. 22. $C_{R,L} \neq 0$ leave equations of motion unchanged, but change boundary conditions (BCs) at $x = 0, L$. Importantly, Heisenberg equations of motion for the quantum flux operators $\hat{\Phi}_j$, $\hat{\Phi}(x, t)$ and $\hat{\Phi}_{R,L}(x, t)$ turn out to be

formally identical to Euler-Lagrange equations for (12) with classical fields promoted to operators.

To express the Heisenberg equations of motion in a compact way, we introduce the following notations. $\Phi_0 \equiv \frac{h}{2e}$ is the superconducting flux quantum and E_j is the Josephson energy. $C_s \equiv C_g C_j / (C_g + C_j)$ is the series capacitance of C_j and C_g and $\gamma \equiv C_g / (C_g + C_j)$. There is a modified capacitance per unit length in the resonator due to the coupling to the transmon qubit at position x_0 :

$$c(x, x_0) \equiv c + C_s \delta(x - x_0). \quad (13)$$

c and l are the capacitance and inductance per unit length in the resonator and the waveguides.

We pass to unitless coordinates and operators ($v_p \equiv 1/\sqrt{lC}$)

$$\begin{aligned} x &\rightarrow \frac{x}{L}, \quad t \rightarrow \frac{t}{\frac{L}{v_p}}, \quad \omega \rightarrow \frac{\omega}{v_p} L, \\ \hat{\varphi} &\equiv 2\pi \frac{\hat{\Phi}}{\Phi_0}, \quad \hat{n} \equiv \frac{\hat{Q}}{2e} \end{aligned} \quad (14)$$

The newly introduced operators $\hat{\varphi}$ and \hat{n} represent phase and number and are canonically conjugate: $[\hat{\varphi}_j, \hat{n}_j] = i$ and $[\hat{\varphi}(x, t), \hat{n}(x', t')] = i\delta(x - x')\delta(t - t')$. Below we use unitless capacitances $\chi_i \equiv C_i / (cL)$, $i = R, L, j, g, s$, and the unitless capacitance per unit length becomes

$$\chi(x, x_0) \equiv 1 + \chi_s \delta(x - x_0). \quad (15)$$

In terms of the quantities introduced, the Heisenberg equations of motion for the superconducting phase operators are:

$$\hat{\varphi}_j(t) + (1 - \gamma)\omega_j^2 \sin[\hat{\varphi}_j(t)] = \gamma \partial_t^2 \hat{\varphi}(x_0, t), \quad (16a)$$

$$[\partial_x^2 - \chi(x, x_0)\partial_t^2] \hat{\varphi}(x, t) = \chi_s \omega_j^2 \sin[\hat{\varphi}_j(t)] \delta(x - x_0), \quad (16b)$$

$$\partial_x^2 \hat{\varphi}_{R,L}(x, t) - \partial_t^2 \hat{\varphi}_{R,L}(x, t) = 0, \quad (16c)$$

with boundary conditions

$$\begin{aligned} -\partial_x \hat{\varphi}|_{x=1^-} &= -\partial_x \hat{\varphi}_R|_{x=1^+} \\ &= \chi_R \partial_t^2 [\hat{\varphi}(1^-, t) - \hat{\varphi}_R(1^+, t)], \end{aligned} \quad (17a)$$

$$\begin{aligned} -\partial_x \hat{\varphi}|_{x=0^+} &= -\partial_x \hat{\varphi}_L|_{x=0^-} \\ &= \chi_L \partial_t^2 [\hat{\varphi}_L(0^-, t) - \hat{\varphi}(0^+, t)], \end{aligned} \quad (17b)$$

$$\hat{\varphi}(x = x_0^-, t) = \hat{\varphi}(x = x_0^+, t), \quad (17c)$$

$$\begin{aligned} \partial_x \hat{\varphi}|_{x=x_0^+} - \partial_x \hat{\varphi}|_{x=x_0^-} - \chi_s \partial_t^2 \hat{\varphi}(x_0, t) \\ = \chi_s \omega_j^2 \sin[\hat{\varphi}_j(t)]. \end{aligned} \quad (17d)$$

In Eqs. (16a) and (16b), the oscillation frequency is unitless $\omega_j^2 = 8\mathcal{E}_c \mathcal{E}_j$, in terms of unitless Josephson and charging energies

$$\mathcal{E}_{j,c} \equiv \sqrt{lC} L \frac{E_{j,c}}{\hbar}, \quad E_c \equiv \frac{e^2}{2C_j}. \quad (18)$$

Equations (16a-16b) are Eqs. (2-3) in the main text.

II. SPECTRAL REPRESENTATION OF THE GREEN'S FUNCTION

In this section we introduce a spectral representation of the Green's function. The Green's function enters the effective Heisenberg equation of motion for the superconducting phase of the transmon qubit (see Ref. 24 for a complete derivation). The resonator Green's function appears if one follows this aim in Eqs. (16a) and (16b): one has to solve for $\hat{\varphi}(x, t)$, which is driven by the qubit in Eq. (16b), and substitute into (16a). The resonator Green's function is defined as the response of the resonator fields, described by the left hand sides of Eqs. (16b-16c), to a δ -function source in space-time

$$[\partial_x^2 - \chi(x, x_0)\partial_t^2]G(x, t|x_0, t_0) = \delta(x - x_0)\delta(t - t_0), \quad (19)$$

obeying BCs (17a-17c) with $\hat{\varphi}(x, t)$ replaced by $G(x, t|x_0, t_0)$. Introducing Fourier transforms

$$\tilde{G}(x, x_0, \omega) = \int_{-\infty}^{\infty} dt G(x, t|x_0, t_0) e^{+i\omega(t-t_0)}, \quad (20a)$$

$$G(x, t|x_0, t_0) = \int_{-\infty}^{\infty} \frac{d\omega}{2\pi} \tilde{G}(x, x_0, \omega) e^{-i\omega(t-t_0)}, \quad (20b)$$

Equation (19) becomes a Helmholtz equation

$$[\partial_x^2 + \omega^2\chi(x, x_0)]\tilde{G}(x, x_0, \omega) = \delta(x - x_0). \quad (21)$$

while the BCs (17a-17c) are transformed by replacing $\partial_t \rightarrow -i\omega$ to

$$\begin{aligned} \partial_x \tilde{G} \Big|_{x=1^-} &= \partial_x \tilde{G} \Big|_{x=1^+} \\ &= \chi_R \omega^2 \left(\tilde{G} \Big|_{x=1^-} - \tilde{G} \Big|_{x=1^+} \right), \end{aligned} \quad (22a)$$

$$\begin{aligned} \partial_x \tilde{G} \Big|_{x=0^-} &= \partial_x \tilde{G} \Big|_{x=0^+} \\ &= \chi_L \omega^2 \left(\tilde{G} \Big|_{x=0^-} - \tilde{G} \Big|_{x=0^+} \right). \end{aligned} \quad (22b)$$

$$\tilde{G} \Big|_{x=x_0^+} = \tilde{G} \Big|_{x=x_0^-}, \quad (22c)$$

$$\partial_x \tilde{G} \Big|_{x=x_0^+} - \partial_x \tilde{G} \Big|_{x=x_0^-} + \chi_s \omega^2 \tilde{G} \Big|_{x=x_0} = 1, \quad (22d)$$

Lastly, outgoing BCs at infinity model the baths:

$$\partial_x \tilde{G}(x, x_0, \omega) \Big|_{x \rightarrow \pm\infty} = \pm i\omega \tilde{G}(x \rightarrow \pm\infty, x_0, \omega). \quad (23)$$

Excitations leaving the resonator never reflect back towards it.

A. Spectral representation of Green's function for $\chi_{R,L} = 0$

Setting $\chi_R = \chi_L = 0$ (amounting to a closed resonator) imposes Neumann BC $\partial_x \tilde{G}|_{x=0,1} = 0$ and the

problem for \tilde{G} is Hermitian. \tilde{G} can be expanded in terms of a discrete set of normal modes satisfying

$$\partial_x^2 \tilde{\varphi}_n(x) + \chi(x, x_0)\omega_n^2 \tilde{\varphi}_n(x) = 0, \quad (24a)$$

$$\partial_x \tilde{\varphi}_n(x) \Big|_{x=0,1} = 0. \quad (24b)$$

An important feature of the modes is that their derivative is discontinuous

$$-\partial_x \tilde{\varphi}_n(x) \Big|_{x_0^-}^{x_0^+} = \chi_s \omega_n^2 \tilde{\varphi}_n(x_0), \quad (25)$$

Physically, this is the continuity equation at x_0 , or current conservation. The mode amplitude at x_0 is suppressed. These observations lead us to name this set of resonator eigenmodes the *current-conserving (CC) basis*.

The CC basis eigenfrequencies obey a transcendental equation

$$\sin(\omega_n) + \chi_s \omega_n \cos(\omega_n x_0) \cos[\omega_n(1 - x_0)] = 0, \quad (26)$$

while the eigenfunctions read

$$\tilde{\varphi}_n(x) \propto \begin{cases} \cos[\omega_n(1 - x_0)] \cos(\omega_n x), & 0 < x < x_0 \\ \cos(\omega_n x_0) \cos[\omega_n(1 - x)], & x_0 < x < 1 \end{cases} \quad (27)$$

and the basis is orthonormal over $[0, 1]$:

$$\int_0^1 dx \chi(x, x_0) \tilde{\varphi}_m(x) \tilde{\varphi}_n(x) = \delta_{mn}. \quad (28)$$

Equation (26) can be solved numerically or asymptotically as $n \rightarrow \infty$, as we do in Sec. V.

The spectral representation of $\tilde{G}(x, x', \omega)$ [37–39] is

$$\tilde{G}(x, x', \omega) = \sum_{n \in \mathbb{N}} \frac{\tilde{\varphi}_n(x) \tilde{\varphi}_n(x')}{\omega^2 - \omega_n^2} = \sum_{\substack{n \in \mathbb{Z} \\ n \neq 0}} \frac{1}{2\omega} \frac{\tilde{\varphi}_n(x) \tilde{\varphi}_n(x')}{\omega - \omega_n}, \quad (29)$$

since $\omega_{-n} = -\omega_n$ and $\tilde{\varphi}_{-n}(x) = \tilde{\varphi}_n(x)$.

B. Spectral representation of Green's function for $\chi_{R,L} \neq 0$

If the resonator is open, $\chi_{L,R} \neq 0$, we resort to a spectral representation in terms of a discrete set of non-Hermitian modes [24] that carry constant flux away from the resonator, Constant Flux (CF) modes [40]. CF modes satisfy the homogeneous wave equation

$$\partial_x^2 \tilde{\varphi}_n(x, \omega) + \chi(x, x_0)\omega_n^2(\omega) \tilde{\varphi}_n(x, \omega) = 0, \quad (30)$$

with BCs (22a)-(22c) and (23). Both the modes $\tilde{\varphi}_n(x, \omega)$ and their frequencies $\omega_n(\omega)$ depend on the source frequency ω .

An outgoing plane wave solution for the left and right waveguides obeying (23), is

$$\tilde{\varphi}_n(x, \omega) = \begin{cases} A_n^< e^{i\omega_n(\omega)x} + B_n^< e^{-i\omega_n(\omega)x}, & 0 < x < x_0 \\ A_n^> e^{i\omega_n(\omega)x} + B_n^> e^{-i\omega_n(\omega)x}, & x_0 < x < 1 \\ C_n e^{i\omega x}, & x > 1 \\ D_n e^{-i\omega x}, & x < 0 \end{cases} \quad (31)$$

Applying BCs (22c-22b) leads to a transcendental equation analogous to the closed case which fixes the parametric dependence $\omega_n(\omega)$ [24].

The CF modes satisfy now a biorthonormality [40] condition

$$\int_0^1 dx \chi(x, x_0) \tilde{\varphi}_m^*(x, \omega) \tilde{\varphi}_n(x, \omega) = \delta_{mn}, \quad (32)$$

where $\{\tilde{\varphi}_m(x, \omega)\}$ obey the Hermitian adjoint of (30). $\tilde{\varphi}_n(x, \omega)$ and $\tilde{\varphi}_n^*(x, \omega)$ are right and left eigenfunctions and obey $\tilde{\varphi}_n(x, \omega) = \tilde{\varphi}_n^*(x, \omega)$.

The CF mode spectral representation of the Green's function of the open resonator is

$$\tilde{G}(x, x', \omega) = \sum_n \frac{\tilde{\varphi}_n(x, \omega) \tilde{\varphi}_n^*(x', \omega)}{\omega^2 - \omega_n^2(\omega)}. \quad (33)$$

There are two sets of poles of $\tilde{G}(x, x', \omega)$ in the complex plane. When the denominator of (33) vanishes, $\omega = \omega_n(\omega)$, which corresponds to quasi-bound eigenfrequencies that obey

$$\begin{aligned} & [e^{2i\omega_n} - (1 - 2i\chi_L\omega_n)(1 - 2i\chi_R\omega_n)] \\ & + \frac{i}{2}\chi_s\omega_n[e^{2i\omega_n x_0} + (1 - 2i\chi_L\omega_n)] \\ & \times [e^{2i\omega_n(1-x_0)} + (1 - 2i\chi_R\omega_n)] = 0. \end{aligned} \quad (34)$$

The solutions reside in the lower half of complex ω -plane and come in symmetric pairs with respect to the $\Im\{\omega\}$ axis, i.e. if ω_n satisfies (34), so does $-\omega_n^*$. Therefore the eigenfrequencies are

$$\omega_n = \begin{cases} -i\kappa_0, & n = 0 \\ +\nu_n - i\kappa_n, & n \in +\mathbb{N} \\ -\nu_n - i\kappa_n, & n \in -\mathbb{N} \end{cases} \quad (35)$$

where $\nu_n > 0$ and $\kappa_n > 0$ are the oscillation frequency and decay rates of quasi-bound mode n , respectively. The dependence of κ_n on mode number n is plotted in Fig. 2 of the main letter. Note the existence of a pole at $\omega = 0$, which comes from the ω -dependence of CF states $\tilde{\varphi}_n(x, \omega)$ [40].

III. MULTIMODE JAYNES-CUMMINGS HAMILTONIAN

The classical Hamiltonian for the cQED system can be found from the circuit Lagrangian (12) [22]

$$\begin{aligned} \mathcal{H}_{sys} &= 4\mathcal{E}_c n_j^2(t) - \mathcal{E}_j \cos[\varphi_j(t)] \\ &+ \int_0^1 dx \left\{ \frac{n^2(x, t)}{2\chi(x, x_0)} + \frac{1}{2} [\partial_x \varphi(x, t)]^2 \right\} \\ &+ 2\pi\gamma z n_j(t) \int_0^1 dx \frac{n(x, t)}{\chi(x, x_0)} \delta(x - x_0), \end{aligned} \quad (36)$$

where $z \equiv Z/R_Q$ where $Z \equiv \sqrt{l/c}$ is the characteristic impedance of the resonator and $R_Q \equiv h/(2e)^2$ is the superconducting resistance quantum. The modification in capacitance per length originates from the system Lagrangian that contains the gauge-invariant qubit-resonator coupling $\chi_g[\dot{\varphi}_j(t) - \dot{\varphi}(x_0, t)]^2/2$. In contrast, a phenomenological product coupling $\chi_g \dot{\varphi}_j(t) \dot{\varphi}(x_0, t)$ would yield a \mathcal{H}_{sys} with $\chi_s = 0$ which results in bare resonator modes.

For the purpose of quantizing \mathcal{H}_{sys} , we find the spectrum of the resonator by solving the corresponding Helmholtz eigenvalue problem that has been discussed in Sec. (II A). We find

$$\begin{aligned} \hat{\mathcal{H}}_{sys} &\equiv \frac{\omega_j}{4} \left\{ \hat{\mathcal{Y}}_j^2 - \frac{\sqrt{2}}{\epsilon} \cos[(2\epsilon^2)^{1/4} \hat{\mathcal{X}}_j] \right\} \\ &+ \sum_n \left\{ \frac{\nu_n}{4} [\hat{\mathcal{X}}_n^2 + \hat{\mathcal{Y}}_n^2] + g_n \hat{\mathcal{Y}}_j \hat{\mathcal{Y}}_n \right\}, \end{aligned} \quad (37)$$

where we have defined the canonically conjugate variables $\hat{\mathcal{X}}_l \equiv (\hat{a}_l + \hat{a}_l^\dagger)$ and $\hat{\mathcal{Y}}_l \equiv -i(\hat{a}_l - \hat{a}_l^\dagger)$, where \hat{a}_l represent the boson annihilation operator of sector $l \equiv j, c$. Moreover, $\omega_j \equiv \sqrt{8\mathcal{E}_j\mathcal{E}_c}$ and $\epsilon \equiv \sqrt{\mathcal{E}_c/\mathcal{E}_j}$ is a measure for the strength of transmon nonlinearity. For $\epsilon = 0$, we recover $\omega_j(\hat{\mathcal{X}}_j^2 + \hat{\mathcal{Y}}_j^2)/4$, the Hamiltonian of a simple harmonic oscillator. In the transmon regime where $\epsilon \ll 1$, the leading contribution is $-\sqrt{2}\epsilon\omega_j\hat{\mathcal{X}}_j^4/48$. The coupling between qubit and the n th CC mode of the resonator is

$$g_n = \frac{1}{2}\gamma\sqrt{\chi_j}\sqrt{\omega_j\nu_n}\tilde{\varphi}_n(x_0). \quad (38)$$

There are typically two approaches to diagonalize Eq. (37). In the first approach, assuming that the qubit nonlinearity is strong, one performs a two level reduction. Then, the multimode Rabi Hamiltonian can be derived from Eq. (37) by projecting the quadratures to Pauli sigma matrices, $\hat{\mathcal{X}}_j \rightarrow \hat{\sigma}^x$ and $\hat{\mathcal{Y}}_j \rightarrow \hat{\sigma}^y$, which yields

$$\begin{aligned} \hat{\mathcal{H}}_{Rabi} &= \frac{\omega_j}{2} \hat{\sigma}^z + \sum_n \nu_n \hat{a}_n^\dagger \hat{a}_n \\ &- \sum_n g_n (\hat{a}_n - \hat{a}_n^\dagger) (\hat{\sigma}^- - \hat{\sigma}^+). \end{aligned} \quad (39)$$

In the rotating wave approximation, Eq. (39) transforms into the multimode Jaynes-Cummings Hamiltonian

$$\hat{\mathcal{H}}_{\text{JC}} = \frac{\omega_j}{2} \hat{\sigma}^z + \sum_n \nu_n \hat{a}_n^\dagger \hat{a}_n + \sum_n g_n (\hat{\sigma}^+ \hat{a}_n + \hat{\sigma}^- \hat{a}_n^\dagger) \quad (40)$$

used in the main text. Analytic results can be found for the Purcell decay rate and the Lamb shift in the dispersive limit where $g_n \ll |\omega_j - \omega_n|$ [10]. In a Lindblad calculation, resonator losses are included by a Bloch-Redfield approach through the Master equation for the reduced density matrix of the resonator and qubit degrees of freedom $\dot{\hat{\rho}} = -i[\hat{\mathcal{H}}_{\text{JC}}, \hat{\rho}] + \frac{\kappa_n}{2} (2\hat{a}_n \hat{\rho} \hat{a}_n^\dagger - \{\hat{\rho}, \hat{a}_n^\dagger \hat{a}_n\})$, where κ_n can be replaced from the solutions to Eq. (34). The second approach treats the nonlinearity as a weak perturbation and is explained in the next section.

IV. WEAKLY NONLINEAR TRANSMON

In this section we summarize the steps necessary to derive Eq. (10) of the main text. The full development of multi scale perturbation theory is in Ref. 24. By keeping the lowest order nonlinearity (Kerr terms which are quartic in the transmon quadrature), the Hamiltonian can be rewritten in a new basis that diagonalizes the quadratic part

$$\begin{aligned} \hat{\mathcal{H}}_{\text{sys}} \equiv & \frac{\beta_j}{4} (\hat{\mathcal{X}}_j^2 + \hat{\mathcal{Y}}_j^2) + \sum_n \frac{\beta_n}{4} (\hat{\mathcal{X}}_n^2 + \hat{\mathcal{Y}}_n^2) \\ & - \frac{\varepsilon \omega_j}{8} \left(u_j \hat{\mathcal{X}}_j + \sum_n u_n \hat{\mathcal{X}}_n \right)^4, \end{aligned} \quad (41)$$

where $\varepsilon \equiv \sqrt{2}\epsilon/6$, $\beta_{j,n}$ are hybridized frequencies and $u_{j,n}$ are hybridization coefficients: $\hat{\mathcal{X}}_j = u_j \hat{\mathcal{X}}_j + \sum_n u_n \hat{\mathcal{X}}_n$.

The Heisenberg equations of motion for quadratures become a set of quantum Duffing equations coupled via the quartic terms

$$\hat{\mathcal{X}}_l(t) + \beta_l^2 \left\{ \hat{\mathcal{X}}_l(t) - \varepsilon_l \left[u_j \hat{\mathcal{X}}_j(t) + \sum_n u_n \hat{\mathcal{X}}_n(t) \right]^3 \right\} = 0, \quad (42)$$

where $\varepsilon_l \equiv \frac{\omega_j}{\beta_l} u_l \varepsilon$ for $l \equiv j, n$. Up to lowest order in the perturbation [24], we find an operator valued correction of the linear theory qubit-like frequency β_j :

$$\hat{\beta}_j = \beta_j - \frac{\sqrt{2}\epsilon}{4} \omega_j \left[u_j^4 \hat{\mathcal{H}}_j(0) + \sum_n 2u_j^2 u_n^2 \hat{\mathcal{H}}_n(0) \right], \quad (43a)$$

and an analogous correction of the resonator like fre-

quency β_n as

$$\begin{aligned} \hat{\beta}_n = \beta_n - \frac{\sqrt{2}\epsilon}{4} \omega_j \left[u_n^4 \hat{\mathcal{H}}_n(0) + 2u_n^2 u_j^2 \hat{\mathcal{H}}_j(0) \right. \\ \left. + \sum_{m \neq n} 2u_n^2 u_m^2 \hat{\mathcal{H}}_m(0) \right], \end{aligned} \quad (43b)$$

where $\hat{\mathcal{H}}_l(0) \equiv \frac{1}{4} [\hat{\mathcal{X}}_l^2(0) + \hat{\mathcal{Y}}_l^2(0)]$ for $l = j, n$. In the main text, Eq. (10), the bar notation is dropped. The lowest order MSPT solution for the qubit quadrature becomes, in terms of renormalized frequencies $\hat{\beta}_{j,n}$, [24]

$$\begin{aligned} \hat{\mathcal{X}}_j^{(0)}(t) = & u_j \frac{\hat{a}_j(0) e^{-i\hat{\beta}_j t} + e^{-i\hat{\beta}_j t} \hat{a}_j(0)}{2 \cos\left(\frac{3\omega_j}{4} u_j^4 \varepsilon t\right)} + H.c. \\ & + \sum_n \left[u_n \frac{\hat{a}_n(0) e^{-i\hat{\beta}_n t} + e^{-i\hat{\beta}_n t} \hat{a}_n(0)}{2 \cos\left(\frac{3\omega_j}{4} u_n^4 \varepsilon t\right)} + H.c. \right]. \end{aligned} \quad (44)$$

This equation takes into account corrections up to $\mathcal{O}(\varepsilon)$ in frequencies. To extract these corrections, we must evaluate the expectation value of Eq. (44) with respect to the initial density matrix. We chose $\hat{\rho} = |\Psi\rangle_j \langle \Psi|_j \otimes |0\rangle_{\text{ph}} \langle 0|_{\text{ph}}$ with $|\Psi\rangle_j = (|0\rangle_j + |1\rangle_j)/\sqrt{2}$. The correction to the transmon like frequency is obtained from the Fourier components of $\langle \hat{\mathcal{X}}_j(t) \rangle$. This is the correction plotted in Fig. 3 of the main text.

V. ASYMPTOTIC BEHAVIOR OF LIGHT-MATTER COUPLING

In this section we find the asymptotic behavior of the eigenfrequencies ω_n and eigenmodes $\tilde{\varphi}_n(x)$ of the resonator discussed in the main text. This provides an analytical understanding of the high frequency suppression in the light-matter coupling g_n .

To point out the origin of the suppression that arise from a nonzero χ_s , let us consider the closed resonator ($\chi_{R,L} = 0$) case. Consider the special case of $x_0 = 0^+$ first. This is of experimental interest in order to achieve the maximum coupling to all modes of a resonator. Then, the transcendental Eq. (26) simplifies to

$$\sin(\omega_n) + \chi_s \omega_n \cos(\omega_n) = 0, \quad (45)$$

which can be rewritten as

$$\tan(\omega_n) = -\chi_s \omega_n. \quad (46)$$

The large ω_n solution for $\chi_s \neq 0$ is then obtained

$$\lim_{n \rightarrow \infty} \omega_n = n\pi - \frac{\pi}{2}, \quad (47)$$

which is independent of the value for χ_s . This implies that the effect of a nonzero χ_s on ω_n is a total shift $\pi/2$

(half of the free spectral range) in comparison with the case $\chi_s = 0$. Substituting $x_0 = 0^+$ in Eq. (27), the normalization factor \mathcal{N}_n is found via Eq. (28) as

$$\int_0^1 dx \cos^2[\omega_n(1-x)] + \chi_s \cos^2(\omega_n) = \frac{1}{\mathcal{N}_n^2}, \quad (48)$$

which gives

$$\mathcal{N}_n = \frac{\sqrt{2}}{\sqrt{1 + \chi_s \cos^2(\omega_n)}}. \quad (49)$$

Therefore the eigenmode is found as

$$\tilde{\varphi}_n(x_0 = 0^+) = \frac{\sqrt{2} \cos(\omega_n)}{\sqrt{1 + \chi_s \cos^2(\omega_n)}}. \quad (50)$$

Using the trigonometric identity

$$\cos^2(\omega_n) = \frac{1}{1 + \tan^2(\omega_n)} \quad (51)$$

and Eq. (46) we can rewrite Eq. (50) as

$$\tilde{\varphi}_n(x_0 = 0^+) = \frac{\sqrt{2}}{\sqrt{1 + \chi_s + \chi_s^2 \omega_n^2}}, \quad (52)$$

which now provides the algebraic dependence of $\tilde{\varphi}_n(x_0)$ on ω_n . According to Eq. (52), for large enough ω_n ($\chi_s \omega_n \gg 1 + \chi_s$), we find

$$\tilde{\varphi}_n(x_0) \sim \frac{1}{\omega_n}, \quad (53)$$

where the symbol \sim represents asymptotic equivalence. This imposes a natural cut-off on the light matter coupling for $n \rightarrow \infty$, since

$$g_n \propto \sqrt{\omega_n} \tilde{\varphi}_n(x_0) \sim \frac{1}{\sqrt{\omega_n}}. \quad (54)$$

Next, we would like to find the asymptotic behavior of ω_n and $\tilde{\varphi}_n(x_0)$ for a general x_0 . In order to bring Eq. (26) into a similar form to Eq. (46), we first replace $\sin(\omega_n) = \sin[\omega_n x_0 + \omega_n(1-x_0)]$ and then divide by $\cos(\omega_n x_0) \cos[\omega_n(1-x_0)]$ to obtain

$$\tan(\omega_n x_0) + \tan[\omega_n(1-x_0)] = -\chi_s \omega_n. \quad (55)$$

Next, the normalization factor \mathcal{N}_n is found from Eq. (28) as

$$\mathcal{N}_n = \frac{\sqrt{2}}{\sqrt{x_0 \cos^2[\omega_n(1-x_0)] + (1-x_0) \cos^2(\omega_n x_0) + \chi_s \cos^2[\omega_n(1-x_0)] \cos^2(\omega_n x_0)}}, \quad (56)$$

Plugging this into Eq. (27) we find

$$\tilde{\varphi}_n(x_0) = \frac{\sqrt{2}}{\sqrt{1 + \chi_s + x_0 \tan^2(\omega_n x_0) + (1-x_0) \tan^2[\omega_n(1-x_0)]}} \quad (57)$$

Equations (55) and (57) provide the asymptotic behavior of ω_n , $\tilde{\varphi}_n(x_0)$ and g_n for a general x_0 .

($\epsilon = 0$) for $\hat{\mathcal{X}}_{j,n}(t)$ as

$$(d_t^2 + \omega_j^2) \hat{\mathcal{X}}_j(t) = - \sum_n 2g_n \omega_n \hat{\mathcal{X}}_n(t), \quad (58a)$$

$$(d_t^2 + 2\kappa_n d_t + \omega_n^2) \hat{\mathcal{X}}_n(t) = -2g_n \omega_j \hat{\mathcal{X}}_j(t) - \hat{f}_n(t), \quad (58b)$$

VI. CHARACTERISTIC FUNCTION $D_j(s)$ AND ITS CONVERGENCE

In this section we derive the expression for the characteristic function $D_j(s)$ and compare its convergence in number of resonator modes with and without the modification we found for g_n .

Consider the Heisenberg-Langevin equations of motion corresponding to Hamiltonian (37) in the linear regime

where κ_n and \hat{f}_n are the decay rate and noise operator coming from coupling to the waveguide degrees of freedom [41].

Equations (58a-58b) are linear constant coefficient ODEs and can be solved exactly via the unilateral Laplace transform

$$\tilde{h}(s) = \int_0^\infty dt h(t) e^{-st}. \quad (59)$$

Taking the Laplace transform of Eqs. (58a-58b) we ob-

tain

$$(s^2 + \omega_j^2) \hat{\mathcal{X}}_j(s) + \sum_n 2g_n \omega_n \hat{\mathcal{X}}_n(s) = s\hat{\mathcal{X}}_j(0) + \hat{\mathcal{X}}_j(0), \quad (60a)$$

$$(s^2 + 2\kappa_n s + \omega_n^2) \hat{\mathcal{X}}_n(s) + 2g_n \omega_j \hat{\mathcal{X}}_j(s) = (s + 2\kappa_n) \hat{\mathcal{X}}_n(0) + \hat{\mathcal{X}}_n(0) + \hat{f}(s). \quad (60b)$$

The solution for $\hat{\mathcal{X}}_j(s)$ then reads

$$\hat{\mathcal{X}}_j(s) = \frac{\hat{N}_j(s)}{D_j(s)}, \quad (61)$$

where the numerator

$$\hat{N}_j(s) = s\hat{\mathcal{X}}_j(0) + \hat{\mathcal{X}}_j(0) - \sum_n \frac{2g_n \omega_n \left[(s + 2\kappa_n) \hat{\mathcal{X}}_n(0) + \hat{\mathcal{X}}_n(0) - \hat{f}_n(s) \right]}{s^2 + 2\kappa_n s + \omega_n^2}, \quad (62)$$

contains the operator initial conditions and the denominator

$$D_j(s) \equiv s^2 + \omega_j^2 - \sum_n \frac{4g_n^2 \omega_j \omega_n}{s^2 + 2\kappa_n s + \omega_n^2}. \quad (63)$$

is the characteristic function whose roots give the hybridized poles of the full system. Therefore, we can represent $D_j(s)$ as

$$D_j(s) = (s - p_j)(s - p_j^*) \prod_n \frac{(s - p_n)(s - p_n^*)}{(s - z_n)(s - z_n^*)}, \quad (64)$$

where $p_{j,n} \equiv -\alpha_{j,n} - i\beta_{j,n}$ stand for the transmon-like and the n th resonator-like poles, respectively. Furthermore, $z_n \equiv -\kappa_n - i\sqrt{\omega_n^2 - \kappa_n^2}$ is the n th bare non-Hermitian resonator mode. The notation (p for poles and z for zeros) is chosen based on $1/D_j(s)$ that appears in the Laplace solution (61).

In order to compute the hybridized poles in practice, we need to truncate the number of resonator modes in $D_j(s)$. This truncation is only justified if the function $D_j(s)$ converges as we include more and more modes. First, note that without the correction give by χ_s this sum is divergent, since $g_n \sim \sqrt{\omega_n} \sim \sqrt{n}$ and for a fixed s we obtain

$$\frac{4g_n^2 \omega_j \omega_n}{s^2 + 2\kappa_n s + \omega_n^2} \sim \frac{\omega_n^2}{\omega_n^2} \sim 1. \quad (65)$$

Hence, the series is divergent. On the other hand, we found that for a non-zero χ_s , $g_n \sim 1/\sqrt{\omega_n} \sim 1/\sqrt{n}$. Therefore we find

$$\frac{4g_n^2 \omega_j \omega_n}{s^2 + 2\kappa_n s + \omega_n^2} \sim \frac{1}{\omega_n^2} \sim \frac{1}{n^2}, \quad (66)$$

and the series becomes convergent. In writing Eq. (66), we used the fact that $\omega_n \sim n$ and κ_n has a sublinear asymptotic behavior found numerically.

VII. DIVERGENCE IN THE WIGNER-WEISSKOPF THEORY OF SPONTANEOUS EMISSION

Divergence of the Purcell decay rate appears in other frameworks besides the dispersive limit Jaynes-Cummings model as well. In this appendix, we show that the spontaneous decay rate of a qubit coupled to continuum of modes is also *divergent*, unless the gauge invariance of the interaction is incorporated as presented in this manuscript. The impression of an (erroneous) finite decay rate in free space goes back to Wigner and Weisskopf's original work on spontaneous atomic decay, which implicitly makes a Markov approximation (See Sec. 6.3 of [14]). We emphasize that employing the Markov approximation always yields a finite value for the decay rate regardless of the form of spectral function for electromagnetic background.

To see this explicitly, we go over the Wigner-Weisskopf theory of spontaneous emission for a two-level system coupled to a continuum of modes inside an infinitely long 1D medium. In interaction picture, the Hamiltonian reads

$$\hat{\mathcal{H}}_I = \sum_k \hbar \left[g_k^*(x_0) \hat{\sigma}^+ \hat{a}_k e^{i(\omega_j - \omega_k)t} + H.c. \right], \quad (67)$$

which conserves the total number of excitations

$$\hat{N} \equiv \hat{\sigma}^+ \hat{\sigma}^- + \sum_{\vec{k}} \hat{a}_{\vec{k}}^\dagger \hat{a}_{\vec{k}}. \quad (68)$$

As a result, a number conserving Ansatz for the wavefunction can be written as

$$|\Psi(t)\rangle = c_e(t) |e, 0\rangle + \sum_k c_{g,k}(t) |g, 1_k\rangle, \quad (69)$$

where there is either no photon in the cavity and the qubit is in excited state $|e\rangle$, or there is a photon at frequency ω_k with qubit in the ground state $|g\rangle$. By solving the Schrodinger equation we obtain the time evolution of the unknown probability amplitudes $c_e(t)$ and $c_{g,k}(t)$. Combining these equations yields an effective equation for $c_e(t)$ as

$$\dot{c}_e(t) = - \int_0^t dt' \mathcal{K}(t-t') c_e(t'), \quad (70)$$

where the memory Kernel $\mathcal{K}(\tau)$ is given by

$$\mathcal{K}(\tau) \equiv \sum_k |g_k(x_0)|^2 e^{i(\omega_j - \omega_k)\tau}. \quad (71)$$

Next, we replace the expression for $g_k(x_0)$, derived in Sec. III, as

$$|g_k(x_0)|^2 = \frac{\gamma \chi_s}{4} \omega_j \omega_k |\tilde{\varphi}_k(x_0)|^2. \quad (72)$$

Note that without respecting the gauge symmetry of interaction $|\tilde{\varphi}_k(x_0)| = \mathcal{N}(x_0)$ is k -independent. Moreover, the sum over k can be replaced as

$$\sum_k \rightarrow \frac{L}{2\pi} \int_0^\infty dk = \frac{L}{2\pi v_p} \int_0^\infty d\omega_k, \quad (73)$$

for a continuum of modes, where v_p is the phase velocity of the medium. Inserting Eqs. (72) and (73) into the effective Eq. (70) we obtain

$$\begin{aligned} \dot{c}_e(t) = & -\frac{1}{2\pi} \frac{\gamma\chi_s\omega_j\mathcal{N}^2(x_0)L}{4v_p} \\ & \times \int_0^\infty d\omega_k \omega_k \int_0^t dt' e^{i(\omega_j-\omega_k)(t-t')} c_e(t') \end{aligned} \quad (74)$$

Importantly, the integral over ω_k in Eq. (74) does not converge since the integrand grows unbounded as $\omega_k \rightarrow \infty$. To resolve this, Wigner and Weisskopf assumed that the dominant contribution comes from those modes of continuum whose frequency are close to the qubit frequency. Therefore, the factor ω_k can be replaced by ω_j and by extending the lower limit of integral over ω_k to $-\infty$ we can use the identity

$$\int_{-\infty}^{+\infty} d\omega_k e^{i(\omega_j-\omega_k)(t-t')} = 2\pi\delta(t-t'), \quad (75)$$

to arrive at a *finite* value for the spontaneous decay as

$$\dot{c}_e(t) \approx -\frac{\Gamma_{sp}}{2} c_e(t), \quad (76a)$$

$$\Gamma_{sp} \equiv \frac{\gamma\chi_s\omega_j^2\mathcal{N}^2(x_0)L}{2v_p}. \quad (76b)$$

It is worth mentioning that using Markov approximation, one always obtains a finite expression for the spontaneous decay rate regardless of the form for the spectral function.

This happens because instead of integrating over the entire frequency span, the Markov approximation picks a small window around qubit frequency.

Next, we show how our natural high frequency cut-off for light-matter coupling resolves the divergence of Wigner-Weisskopf theory. First, note that applying Markov approximation is indeed unnecessary, since the Volterra Eq. (70) with the memory kernel

$$\mathcal{K}(\tau) = \frac{1}{2\pi} \frac{\gamma\chi_s\omega_j L}{4v_p} \int_0^\infty d\omega_k \omega_k |\tilde{\varphi}_k(x_0)|^2 e^{i(\omega_j-\omega_k)\tau}, \quad (77)$$

has an exact solution in Laplace domain as

$$\tilde{c}_e(s) = \frac{c_e(0)}{s + \tilde{\mathcal{K}}(s)}, \quad (78)$$

where $\tilde{\mathcal{K}}(s) \equiv \int_0^\infty d\tau \mathcal{K}(\tau) e^{-s\tau}$ is the Laplace transform and is found as

$$\tilde{\mathcal{K}}(s) = \frac{1}{2\pi} \frac{\gamma\chi_s\omega_j L}{4v_p} \int_0^\infty d\omega_k \frac{\omega_k |\tilde{\varphi}_k(x_0)|^2}{s + i(\omega_k - \omega_j)}. \quad (79)$$

Second, when the gauge-invariance of the interaction is incorporated, the mode amplitude is frequency dependent that experiences a high frequency suppression as

$$|\tilde{\varphi}_k(x_0)| \sim \frac{1}{\omega_k}. \quad (80)$$

Replacing Eq. (80) into expression (79) for $\tilde{\mathcal{K}}(s)$ we obtain

$$\tilde{\mathcal{K}}(s) \propto \int d\omega_k \frac{1}{\omega_k [s + i(\omega_k - \omega_j)]}. \quad (81)$$

Interestingly, with the corrected expression for the eigenmodes, the integrand behaves like $1/\omega_k^2$ at $\omega_k \rightarrow \infty$, and as a result the integral converges. Otherwise, the integrand behaves like a constant at $\omega_k \rightarrow \infty$ and the result is divergent.

-
- [1] D. Kleppner, Phys. Rev. Lett. **47**, 233 (1981).
[2] P. Goy, J. M. Raimond, M. Gross, and S. Haroche, Phys. Rev. Lett. **50**, 1903 (1983).
[3] R. G. Hulet, E. S. Hilfer, and D. Kleppner, Phys. Rev. Lett. **55**, 2137 (1985).
[4] W. Jhe, A. Anderson, E. A. Hinds, D. Meschede, L. Moi, and S. Haroche, Phys. Rev. Lett. **58**, 666 (1987).
[5] E. M. Purcell, H. C. Torrey, and R. V. Pound, Phys. Rev. **69**, 37 (1946).
[6] W. E. Lamb Jr and R. C. Retherford, Physical Review **72**, 241 (1947).
[7] A. Fragner, M. Göppl, J. Fink, M. Baur, R. Bianchetti, P. Leek, A. Blais, and A. Wallraff, Science **322**, 1357 (2008).
[8] A. A. Houck, J. A. Schreier, B. R. Johnson, J. M. Chow, J. Koch, J. M. Gambetta, D. I. Schuster, L. Frunzio, M. H. Devoret, S. M. Girvin, and R. J. Schoelkopf, Phys. Rev. Lett. **101**, 080502 (2008).
[9] S. E. Nigg, H. Paik, B. Vlastakis, G. Kirchmair, S. Shankar, L. Frunzio, M. H. Devoret, R. J. Schoelkopf, and S. M. Girvin, Phys. Rev. Lett. **108**, 240502 (2012).
[10] M. Boissonneault, J. M. Gambetta, and A. Blais, Phys. Rev. A **79**, 013819 (2009).
[11] S. Filipp, M. Göppl, J. M. Fink, M. Baur, R. Bianchetti, L. Steffen, and A. Wallraff, Phys. Rev. A **83**, 063827 (2011).
[12] M. Malekakhlagh, A. Petrescu, and H. E. Tureci, *Supplementary Material*.
[13] V. Weisskopf and E. Wigner, Zeitschrift für Physik A Hadrons and Nuclei **63**, 54 (1930).

- [14] M. O. Scully and M. S. Zubairy, “*Quantum Optics*” (Cambridge University Press, 1997).
- [15] D. O. Krimer, M. Liertzer, S. Rotter, and H. E. Türeci, Phys. Rev. A **89**, 033820 (2014).
- [16] M. H. Devoret, in *Les Houches, Session LXIII*, Vol. 7, edited by S. Reynaud, E. Giacobino, and J. Zinn-Justin (Elsevier Science, 1997) pp. 351–386.
- [17] W. E. Lamb, R. R. Schlicher, and M. O. Scully, Phys. Rev. A **36**, 2763 (1987).
- [18] J. Koch, T. M. Yu, J. Gambetta, A. A. Houck, D. I. Schuster, J. Majer, A. Blais, M. H. Devoret, S. M. Girvin, and R. J. Schoelkopf, Phys. Rev. A **76**, 042319 (2007).
- [19] J. Schreier, A. A. Houck, J. Koch, D. I. Schuster, B. Johnson, J. Chow, J. M. Gambetta, J. Majer, L. Frunzio, M. H. Devoret, *et al.*, Physical Review B **77**, 180502 (2008).
- [20] M. Devoret, B. Huard, R. Schoelkopf, and L. F. Cugliandolo, eds., “*Quantum Machines: Measurement and Control of Engineered Quantum Systems: Lecture Notes of the Les Houches Summer School: Volume 96, July 2011*” (Lecture Notes of the Les Houches Summer School 96, 2014).
- [21] See also the Supplementary Material for a brief derivation of the Heisenberg-Langevin equation of motion and a discussion of the multimode convergence of its characteristic function, which includes Refs. [10, 14, 20, 22, 24, 35–41].
- [22] M. Malekakhlagh and H. E. Türeci, Phys. Rev. A **93**, 012120 (2016).
- [23] P. W. Milonni, “*The quantum vacuum: an introduction to quantum electrodynamics*” (Academic press, 2013) Chap. 3.
- [24] M. Malekakhlagh, A. Petrescu, and H. E. Türeci, Phys. Rev. A **94**, 063848 (2016).
- [25] J. Bourassa, F. Beaudoin, J. M. Gambetta, and A. Blais, Phys. Rev. A **86**, 013814 (2012).
- [26] We note that this result is valid in the dispersive limit i.e. away from cavity resonances. In that limit, we expect this result to be fairly accurate when compared to the rate extracted from the exact time evolution of the Master equation for the multimode JC model.
- [27] The power law dependence of κ_n and g_n , though universal with respect to χ_s , are specific to the chosen circuit topology.
- [28] A. Caldeira and A. Leggett, Annals of Physics **149**, 374 (1983).
- [29] A. J. Leggett, Phys. Rev. B **30**, 1208 (1984).
- [30] F. Schwabl and W. Thirring, “Quantum theory of laser radiation,” in *Ergebnisse der exakten Naturwissenschaften* (Springer Berlin Heidelberg, Berlin, Heidelberg, 1964) pp. 219–242.
- [31] T. Niemczyk, F. Deppe, H. Huebl, E. P. Menzel, F. Hocke, M. J. Schwarz, J. García-Ripoll, D. Zueco, T. Hämmer, E. Solano, A. Marx, and R. Gross, Nature Physics **6**, 772 (2010).
- [32] C. M. Bender and S. A. Orszag, “*Advanced mathematical methods for scientists and engineers*” (Springer Science & Business Media, 1999).
- [33] C. M. Bender and L. M. A. Bettencourt, Phys. Rev. Lett. **77**, 4114 (1996).
- [34] M. F. Gely, A. Parra-Rodriguez, D. Bothner, Y. M. Blanter, S. J. Bosman, E. Solano, and G. A. Steele, Phys. Rev. B **95**, 245115 (2017).
- [35] L. S. Bishop, arXiv:1007.3520 [cond-mat, physics:quant-ph] (2010).
- [36] A. A. Clerk, M. H. Devoret, S. M. Girvin, F. Marquardt, and R. J. Schoelkopf, Rev. Mod. Phys. **82**, 1155 (2010).
- [37] P. Morse and H. Feshbach, “*Methods of theoretical physics*” (McGraw-Hill, 1953).
- [38] E. N. Economou, “*Green’s functions in quantum physics*”, Vol. 3 (Springer, 1984).
- [39] S. Hassani, “*Mathematical physics: a modern introduction to its foundations*” (Springer Science & Business Media, 2013).
- [40] H. E. Türeci, A. D. Stone, and B. Collier, Phys. Rev. A **74**, 043822 (2006); H. E. Türeci, L. Ge, S. Rotter, and A. D. Stone, Science **320**, 643 (2008).
- [41] I. R. Senitzky, Phys. Rev. **119**, 670 (1960).